Title

The aging slow wave: a shifting amalgam of distinct slow wave and spindle coupling subtypes define slow wave sleep across the human lifespan.

Journal

SLEEP, 44(10)

Authors

McConnell, Brice
Kronberg, Eugene
Teale, Peter
et al.

Publication Date

2021-10-11

DOI

10.1093/sleep/zsab125

Peer reviewed

SLEEPJ, 2021, 1–16

doi: 10.1093/sleep/zsab125
Advance Access Publication Date: 17 May 2021
Original Article

ORIGINAL ARTICLE

The aging slow wave: a shifting amalgam of distinct slow wave and spindle coupling subtypes define slow wave sleep across the human lifespan

Brice V. McConnell[1,*], Eugene Kronberg[1], Peter D. Teale[1], Stefan H. Sillau[1], Grace M. Fishback[1], Rini I. Kaplan[2], Angela J. Fought[3], A. Ranjitha Dhanasekaran[1], Brian D. Berman[4], Alberto R. Ramos[5], Rachel L. McClure[6] and Brianne M. Bettcher[1]

[1]Neurology, University of Colorado, Anschutz Medical Campus, Aurora, CO, USA, [2]Psychological & Brain Sciences, Boston University, Boston, MA, USA, [3]Department of Biostatistics and Informatics, Colorado School of Public Health, Aurora, CO, [4]Neurology, Virginia Commonwealth University, Richmond, VA, USA, [5]Neurology, University of Miami Miller School of Medicine, Miami, FL, USA and [6]Astronomy, University of Wisconsin–Madison, Madison, WI, USA

*Corresponding author. Brice V. McConnell, 12469 E 17th Place, Aurora, CO 80045, USA. Email: brice.mcconnell@cuanschutz.edu.

Abstract

Study Objectives: Slow wave and spindle coupling supports memory consolidation, and loss of coupling is linked with cognitive decline and neurodegeneration. Coupling is proposed to be a possible biomarker of neurological disease, yet little is known about the different subtypes of coupling that normally occur throughout human development and aging. Here we identify distinct subtypes of spindles within slow wave upstates and describe their relationships with sleep stage across the human lifespan.

Methods: Coupling within a cross-sectional cohort of 582 subjects was quantified from stages N2 and N3 sleep across ages 6–88 years old. Results were analyzed across the study population via mixed model regression. Within a subset of subjects, we further utilized coupling to identify discrete subtypes of slow waves by their coupled spindles.

Results: Two different subtypes of spindles were identified during the upstates of (distinct) slow waves: an "early-fast" spindle, more common in stage N2 sleep, and a "late-fast" spindle, more common in stage N3. We further found stages N2 and N3 sleep contain a mixture of discrete subtypes of slow waves, each identified by their unique coupled-spindle timing and frequency. The relative contribution of coupling subtypes shifts across the human lifespan, and a deeper sleep phenotype prevails with increasing age.

Conclusions: Distinct subtypes of slow waves and coupled spindles form the composite of slow wave sleep. Our findings support a model of sleep-dependent synaptic regulation via discrete slow wave/spindle coupling subtypes and advance a conceptual framework for the development of coupling-based biomarkers in age-associated neurological disease.

Statement of Significance

Slow waves of nonrapid eye movement sleep couple with sleep spindles in a process hypothesized to support memory functions. This coupling has recently gained interest as a possible biomarker of cognitive aging and onset of Alzheimer's disease. Most studies have been limited by an assumption that all slow waves (and coupled spindles) are fundamentally the same physiological events. Here we demonstrate that distinct subtypes of slow waves and their coupled spindles can be identified in human sleep. A mixture of different slow wave and spindle subtypes shifts in composition during lighter versus deeper sleep, and aging favors the deep sleep subtypes. These data should inform any future attempts to use slow wave sleep as a biomarker or clinical interventional target.

Key words: slow wave; sleep spindle; memory; coupling; biomarker; EEG

Submitted: 6 July, 2020; **Revised:** 14 March, 2021

Introduction

Slow waves occur during stages N2 and N3 Nonrapid Eye Movement (NREM) sleep and are associated with large-scale synchronization of neuronal populations [1–3]. Spindles are generated and propagated via cortical–thalamic loops, with timing input from the reticular nucleus of the thalamus [4, 5]. In the process of aging, loss of slow waves and sleep spindles is highly correlated with cognitive decline, and abnormal slow wave neuronal circuitry is implicated in the pathogenesis of Alzheimer's disease [6].

The dynamic coordination of slow waves and spindles provides a fundamental framework for synaptic regulation during sleep-dependent memory consolidation [7, 8]. During slow wave sleep, reactivation of memory circuits is hypothesized to be coordinated by spindle oscillations [9–11]. Higher frequency oscillations, termed ripples, are nested within spindles and accompany specific patterns of hippocampal memory reactivation [12–15]. Together, slow waves, spindles and ripples maintain a triple coupling relationship that is proposed to support synaptic plasticity and remodeling of cortical networks during sleep [16–19].

Timing aspects of slow wave and spindle coupling are compromised among aging adults, and abnormal coupling correlates with brain atrophy and deficits in sleep dependent memory performance [8, 20, 21]. Loss of coupling integrity has further been demonstrated to correlate with tau deposition among cognitively intact aging adults, raising the prospects of slow wave and spindle coupling as a possible functional biomarker of early Alzheimer's pathogenesis [22]. Given the role of spindles in regulation of synaptic function [8, 23, 24], an understanding of the pathophysiology of spindle coupling abnormalities may also provide fundamental mechanistic insights into the proposed role of sleep in protecting against neurodegenerative disease [6, 25, 26].

Understanding how the timing aspects of coupling might subserve or modify pathological outcomes is currently limited by an incomplete characterization of the key coupled-event subtypes that occur during neurodevelopment and the aging process. Original descriptions of coupled spindles identified "slow" and "fast" subtypes, occurring before and after the trough of the slow wave downstate, respectively [27, 28]. More recently, human intracranial recordings have also identified additional coupling events during the downstate (pretrough) termed theta bursts, that are proposed to coordinate hippocampal ripples [29, 30] and may trigger slow wave events [31]. During the slow wave upstate (posttrough), discrete spindle subtypes have also been observed within intracranial recordings, with a higher frequency subtype occurring before lower frequency spindles in temporal relation [20, 31, 32]. Little is known about what the timing aspects of these events may signify in the greater context of human sleep and cognitive functions.

Slow wave subtypes have also been proposed, and a model of global slow waves versus local slow waves postulates different neuroanatomical generation of these slow wave subtypes [33, 34]. Global slow waves are hypothesized to be generated via a frontal lobe process, with a predominance in stage N2 sleep. These waves are typically more interspersed rather than tightly clustered and are proposed to include the classically described K-complexes [33, 34]. In contrast, local slow waves are thought to be generated more widely throughout the brain and occur more commonly during N3 sleep [33, 34]. Recent evidence from murine sleep further advances a conceptual model in which a global subtype of slow wave/spindle coupling favors synaptic potentiation, while a distinct local slow wave/spindle coupling subtype drives synaptic downscaling [35]. Despite accumulating evidence that multiple subtypes of slow waves occur in human sleep, it remains unclear how different subtypes of spindles might couple to these different slow waves.

Based on the conceptual framework that coupling integrity is integral to human memory function and a potential biomarker of neurodegenerative disease, we sought to expand the fundamental understanding of coupling physiology by characterizing distinct subtypes of slow wave and spindle coupling across the human lifespan. We tested the hypothesis that subtypes of upstate-specific spindles preferentially occur during different sleep stages, and that predominant upstate coupling subtypes shift throughout neurodevelopment and aging. Further, as a critical step toward elucidating the underlying physiological basis of spindle coupling subtypes, we examined whether coupled spindles could be utilized as an "identification tag" to sort out a mix of different slow wave event subtypes from NREM sleep.

Drawing from 582 subjects aged 6–88 years old from the Cleveland Family Study [36–39], our analyses demonstrate that two subtypes of fast spindle coupling, "early-fast" and "late-fast," can be identified during the upstates of slow waves. By leveraging the wealth of data within this large cross-sectional cohort, we observed that the early-fast coupling subtype preferentially occurs in stage N2 sleep during early life, with a gradual transition to a higher proportion of late-fast coupling subtype as age advances. Meanwhile, the late-fast coupling subtype is the predominant coupling event in stage N3 sleep after early childhood through the later stages of life. We further provide key mechanistic insights by demonstrating that the coupling of spindles can be used to identify discrete populations of slow waves that differ in their association with stage of sleep. Taken together, our findings advance the fundamental conceptual framework of slow wave and spindle coupling and provide key methodological advancements for the development of coupling as a functional biomarker in human neurological disease.

Methods

Participants

Participant data was accessed from the Cleveland Family Study (CFS) via the National Sleep Research Repository [36–39]. The CFS was conducted as a longitudinal study of sleep apnea and included 2284 individuals from 384 families over 16 years of follow-up. All data were collected with written informed consent under protocols approved by a local institutional review board at each institution. Overnight polysomnography recordings were utilized from visit 5 study data for 735 subjects (Figure 1). Data quality was rated by sleep staging experts per standardized study protocol, and EEG recordings with less than 95% overall quality score were excluded from our analysis (n = 132). Recordings with problems noted in differentiating N2 and N3 sleep were also excluded (N = 4), as well as a diagnosis of Parkinson's disease (n = 1), and participants having taken medications for sleep within three days up to the overnight polysomnography (n = 9). An additional seven subjects we excluded due to data quality problems during processing, resulting in 582 subjects for analysis.

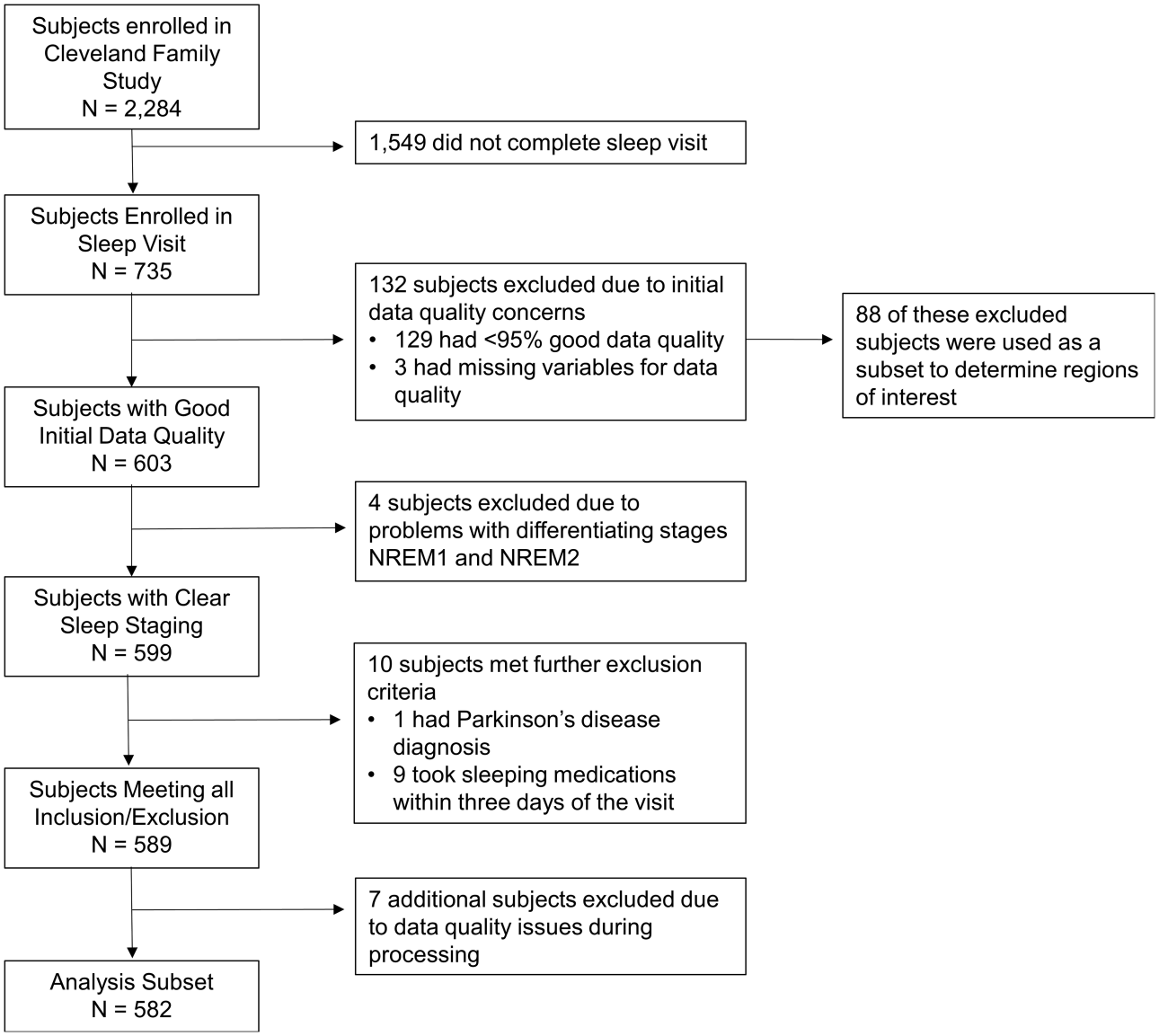

Figure 1. Subject selection flow chart diagram details exclusion criteria.

EEG acquisition

Laboratory-based polysomnography was performed using a 14-channel Compumedics E-Series System (Abbotsford, Australia). EEG was obtained using gold cup electrodes at a sampling rate of 128 Hz (filtered high pass 0.16 Hz and low pass 64 Hz). Scalp electrodes C3 and C4 were referenced to positions A2 and A1, respectively. Recordings were scored by trained technicians at a centralized reading center at Brigham and Women's Hospital in accordance with uniform study protocols and AASM criteria [40].

Spectral analysis

All EEG processing was performed in MATLAB (R2018b; the Mathworks, Inc., Natick, MA) using additional toolboxes including EEGlab [41] and FieldTrip [42]. Multitaper spectral analysis was performed on raw EEG data using discrete prolate slepian sequences as described by Prerau et al [43]. Briefly, data were epoched to 30 s segments with 85% overlap. A frequency range of 0.5 to 30 Hz with a resolution of 0.01 Hz were used to obtain spectral estimates. In total, 29 tapers were created to achieve a frequency smoothing of ±0.5 Hz.

Slow wave detection

Data for slow wave detections were processed from electrodes C3 and C4 from stages N2 and N3 of slow wave sleep, scored by AASM criteria (Supplementary Figure S1) [40]. Notably, the AASM criteria have several well-characterized limitations with regard to consistently classifying N2 versus N3 sleep. Specifically, the distinction between sleep stages is imperfect during transitions between sleep stages [44, 45], and misclassification of N3 sleep may occur among older adults, typically starting midlife with gradual worsening, as their lower-amplitude slow waves cause N3 to be staged as N2 sleep [44]. Despite these known limitations, we utilized AASM criteria for the distinction between N2

and N3 sleep given the predominant application of this method in the current scientific study of sleep, and the lack of a validated alternative method with broad acceptance [44].

Slow waves were identified from combined N2 and N3 sleep EEG segments for each subject for the analyses in Figures 5; Supplementary Figures S8 and S9, and separately for each sleep stage for the remainder of analyses. Slow waves from stage N2 were identified for all subjects. Due to lack of stage N3-specific slow wave events in subjects with minimal or no N3 sleep, we set a minimum of 5% time in N3 (from total sleep) for detection of N3-specific slow waves. The minimum segment of isolated N3 sleep included was 11 min. Sixty-seven subjects did not make sufficient N3 sleep for inclusion of their N3 segments (median age 60.4, IQR 47.6–72.1). Epochs with unscorable data were also excluded from analysis.

Preprocessing for high throughput slow wave identification at the population level was performed via automated artifact reduction (n = 661 subjects, including those used exclusively for time-frequency window [TF-window] determination). Automated management of high amplitude artifacts was accomplished via exclusion of regions of range greater than 900 μV. Remaining raw EEG segments of at least three seconds were detrended; these sections were cut for detrending when the final three seconds exceeded a range of 900 μV. A small cohort was processed for further slow wave and spindle characterization with additional manual visual artifact removal (n = 30 subjects). Manual artifact removal was performed within EEGLAB in 5 s bins with visual inspection and removal of artifacts.

Parameters for slow wave detection were based on prior slow wave/spindle coupling reports [20, 46]. Sequentially, EEG data was detrended to remove any remaining start–end mismatch that would cause ringing and then band-pass filtered in a forward and backward direction (two-pass) using a 6th-order Butterworth filter between 0.16–4 Hz. Zero crossings of the filtered time-series data were identified to detect the beginning of negative and positive half-waves, and candidate slow wave events were identified when zero crossings occurred between 0.5 s and 1 s, or the maximum value of the candidate positive half-wave occurred within 0.5 s from the second zero crossing detection of the negative half-wave (effectively producing a filter for events within 0.5 to 1 Hz frequency range). Minimal and maximal half-wave amplitudes were measured from the zero crossing detections, and slow waves with both positive and negative maximum amplitudes in the top 40% of all waves were selected for subsequent coupling analysis (creating an adaptive amplitude threshold for slow wave event criteria). We rejected all zero crossing pairs with peak/trough amplitudes exceeding four standard deviations from the mean min/max zero crossing pair amplitudes for each subject. The duration (length) of slow waves was measured from the lowest value of the negative half-wave (deepest point of the downstate) to the highest value of the positive half-wave (highest point of the upstate) of identified slow waves for each subject and reported in seconds as an average for characterization of slow wave events. An additional visual inspection was performed on each individual recording's slow wave average composite to ensure correct channel polarity.

Time-frequency analysis

Time-frequency wavelet plots of EEG data were produced to measure coupling of spindles by adapting established methods [20, 27]. An induced power averaging (nonphase-locked power) approach was utilized due to the lack of observed phase locking between spindles to their coupled slow wave events (Supplementary Figure S2). A Morlet-wavelet transformation (8 cycles) was applied to unfiltered EEG regions of 5-seconds for slow wave and baseline segments between 4 Hz and 20 Hz in steps of 0.25 Hz. Given our focus on spindles that are specific to slow wave coupling, we accounted for ongoing "baseline" EEG activity that is observed to contain numerous uncoupled spindles and prominent raw EEG power overlapping with spindle frequencies [27, 32, 46] (illustrated in Supplementary Figure S2). For each 5-second region surrounding the centered trough of a slow wave, a baseline region of matching time length was selected from the interval immediately preceding a run of slow wave (segments containing slow waves were excluded). The mean of these combined baseline regions was used to normalize the resulting amplitude of the mean Morlet-wavelet transformation of all slow wave event regions for each subject. A manual inspection of each time-frequency map was performed to remove any time-frequency maps from analysis that contained ringing artifacts secondary to bandpass filtering (<7% excluded total; <2.5% excluded from any 10 y age increment). As an additional validation of our baseline selection method, we cross-validated the ability to detect peri-slow wave events using a fundamentally different baseline selection method among a randomly selected subset of subjects (ages 20–21, n = 10, ages 40–41, n = 10, and ages 60–61, n = 10). For this subset, we used the entire artifact-free and sleep stage-specific recording segment as baseline, without any separation of slow wave event segments from nonevent EEG segments. This nonselective method was contrasted to the event-free baseline selection method for the same subjects to demonstrate that the potential influence of age-specific baseline selection bias is minimal, while inclusion of slow waves into the baseline predictably decreases the normalized EEG power that is specific to slow wave events (Supplementary Figure S3).

TF-window selection

Regions within the time-frequency wavelet plots were selected for quantitative analysis utilizing a subset of 88 subjects (ages 15–64) from the Cleveland Family Study (Supplementary Table S1). These subjects were noted to have between 75%–95% good EEG data quality, and thus were excluded from our main analysis cohort and restricted to our efforts to define the boundaries of TF-windows. An average composite of slow wave-centered time-frequency wavelet maps from channel C3 was created for all 88 subjects, and four regions of interest were manually selected for subsequent statistical analysis of the main cohort (Supplementary Figure S4). These regions include preslow wave trough activity corresponding to possible theta burst [29–31] and slow spindle activity [27, 47, 48]. The postslow wave trough demonstrates coupling activity consistent with previously described "faster" and "slower" spindles of the slow wave upstate [31, 32], herein referred to as early-fast spindles and late-fast spindles. Within our TF-windows, theta bursts were defined by a TF-window defined between 4 Hz and 5.5 Hz at –0.7 s to 0.5 s from the average slow wave trough, plus an additional region 5.5 Hz to 7 Hz at –0.5 s to 0.4 s from the trough. Pretrough slow spindle TF-window was defined as 7 Hz to 11 Hz, and –0.4 s to 0.2 s from the average trough. Early-fast spindle TF-window was defined as 14 Hz to 17 Hz and 0.1 s to 0.7 s from the average

trough. Late-fast spindle TF-window was defined as 10 Hz to 14 Hz, and 0.4 s to 1.1 s from the average slow wave trough (Supplementary Figure S4).

Notably, we specifically defined spindle events and theta bursts with respect to coupled slow wave relationships in time and frequency space. While previous reports have described slow spindle and fast spindle activity with regard to peaks of raw EEG power during NREM sleep [27, 49], here we sought to disentangle the numerous uncoupled spindles (and their prominent power peaks within the raw EEG; see Supplementary Figure S2) from the specific coupling of spindles with slow waves. An additional illustrative example is provided among a randomly selected subset of subjects (ages 20–21, $n = 10$, ages 40–41, $n = 10$, and ages 60–61, $n = 10$) to demonstrate age-dependent changes in sleep stage-specific power spectra, further supporting the need to account for uncoupled spindle activity by normalizing the slow wave-specific EEG segments to the averaged baseline EEG activity for each subject (Supplementary Figure S5).

Slow wave separation by region of interest spindle EEG power

Normalized EEG power from TF-windows corresponding to the early-fast and late-fast spindles were utilized to separate and sort the total collection of slow waves into two subgroups. Each slow wave was sorted by calculating a ratio of the EEG power values in the corresponding early-fast and late-fast spindle TF-windows. Given unknown prevalence of each slow wave subtype, here we modeled an approximate 50/50 mix of slow wave subtypes based on the early-fast spindle TF-window percentage (early-fast/[early-fast + late-fast]*100) values that were estimated to range from 51.2% to 48.6% across the study population. Using these study-specific parameters, all of the identified slow waves were sorted by top 50% of early-fast spindle TF-window power ratio (early-fast/late-fast) vs top 50% of late-fast spindle power (late-fast/early-fast).

Slow wave separation by co-identification of spindle events and timing alignment

Spindles were identified from combined N2 and N3 sleep EEG segments for each subject. Parameters for spindle detection were based on prior slow wave/spindle coupling reports [27, 50]. Sequentially, artifact free EEG data was detrended and bandpass filtered in a forward and backward direction using a 3rd-order Butterworth filter between 10–14 Hz for late-fast spindles, and between 14.5–17.5 Hz for early-fast spindles. Next the upper spindle envelopes were calculated and an amplitude threshold of 75% percentile of the root mean squared value (of the entire artifact-free and sleep stage-specific recording segments), with a length window of 0.5 s to 3.0 s was used to define spindle events. An absolute threshold of 40 μV in range was used to eliminate artifacts and then only waves within eight standard deviations from the mean amplitude values were used in further analysis. Each spindle event was indexed with respect to adjacent spindle events to determine their ordering. Slow wave events coupled to these populations of spindles were identified by their colocalization within −0.5 to 1.5 s from the trough of a slow wave. These individual slow waves that coupled to each spindle type (late-fast and early-fast) in the time domain were then selected for additional analysis as coupled events of interest.

Statistical analysis

All statistical modeling was performed with SAS v9.4 (SAS Institute Inc., Cary, NC). Normalized EEG power values were obtained from time-frequency wavelet plots within each of the four TF-windows (early-fast, late-fast, slow, and theta) that were defined *a priori*. The TF-window values for each measurement were statistically weighted by the number of slow wave events that were utilized to calculate each corresponding value. To evaluate the relationship with power from each TF-window and age, splines were used to find knots at ages 20 and 60 for characterizing different neurologic stages of life (childhood/adolescence ages 6–20, young adulthood through late-adulthood ages 21–60, and late age 61 and above). Our main power outcome was the percentage of early-fast spindle power within the slow wave upstate (early-fast TF-window divided by the sum of early-fast and late-fast TF-windows, times 100).

Mixed models were used to account for repeated measures from combinations of the electrode (C3 and C4) and stage (N2 and N3), adjusting for sex, sleep apnea (using a binary threshold at 15 apneas and hypopneas with ≥3% oxygen desaturation or arousal per hour of sleep), and age as piece-wise continuous with flex points determined by the knots at 20 and 60, driven by the spline analysis (statistical models with 95% confidence intervals are illustrated in Supplementary Figure S6; dot plots are illustrated in Supplementary Figure S7). Interactions with stage, electrode, and electrode and stage were included for each covariate (early-fast, late-fast, slow, and theta). In each model, we accounted for familial clustering by including family identification number as a random effect. An additional model, stratified by electrode, similarly accounted for repeated measures with the same covariates and interactions, and in this case outcomes were log-transformed normalized EEG power with a covariate specifying the corresponding TF-window (early-fast, late-fast, slow, and theta). Linear combinations of the model parameters were constructed and tested with t and F tests, with estimates and confidence intervals for individual linear combinations. Notably, statistical modeling was performed for both C3 and C4 electrodes, and here we report C3 because we did not identify statistically significant differences when estimates were compared between electrodes for the main outcomes (statistical models for electrodes C3 and C4 are both graphed in Supplementary Figure S6).

Results

Multiple peri-slow wave events can be identified within the downstates and upstates of slow waves via time-frequency analysis of overnight surface EEG recordings

To understand the changes in slow wave coupling that occur across the human lifespan, we created an average of peri-slow wave EEG activity from a cohort of 582 subjects (ages 6–88; Table 1). At time points just before the slow wave trough (slow wave downstate), we observed activity within time-frequency windows (TF-windows) that correspond to previously described

Table 1. Demographics of the study population and the subsets of subjects that were examined for separation of slow wave and spindle subtype analyses

						Age 20–21		Age 40–41		Age 60–61	
	Characteristic	N	N (%) or median (IQR)		Characteristic	N	N (%) or median (IQR)	N	N (%) or median (IQR)	N	N (%) or median (IQR)
Entire study population	Age	582	43.01 (22.20–54.79)	Study subset	–	–	–	–	–	–	–
	Sex	582			Sex	10		10		10	
	- Female		321 (55.15)		- Female		4 (40.00)		5 (50.00)		6 (60.00)
	- Male		261 (44.85)		- Male		6 (60.00)		5 (50.00)		4 (40.00)
	Race	582			Race	10					
	- White		237 (40.72)		- White		3 (30.00)		3 (30.00)		7 (70.00)
	- Black		324 (55.67)		- Black		7 (70.00)		7 (70.00)		3 (30.00)
	- Other		21 (3.61)								
	Apnea Hypopnea Index	582	4.71 (1.47 – 14.14)		Apnea Hypopnea Index	10	2.07 (1.05 – 13.02)	10	5.01 (3.28 – 29.90)	10	12.54 (5.54 – 33.73)
	Apnea Hypopnea	582			Apnea Hypopnea	10		10		10	
	- Less than 15		446 (76.63)		- Less than 15		8 (80.00)		7 (70.00)		6 (60.00)
	- 15 or greater		136 (23.37)		- 15 or greater		2 (20.00)		3 (30.00)		4 (40.00)
	% Time in Stage 1	575	4.13 (2.57 – 6.03)		% Time in Stage 1	10	3.14 (2.03 – 5.51)	10	4.38 (3.77 – 4.77)	10	4.87 (2.90 – 5.65)
	% Time in Stage 2	582	55.30 (47.70 – 64.20)		% Time in Stage 2	30	57.40 (41.40 – 60.50)	10	63.25 (55.10 – 71.40)	10	53.15 (49.40 – 71.80)
	% Time in Stage 3	582	19.85 (12.10 – 28.20)		% Time in Stage 3	30	20.55 (14.0 – 23.0)	10	15.75 (13.30 – 17.90)	10	13.10 (4.61 – 28.60)
	% Time in REM	580	18.25 (14.00 – 22.60)		% Time in REM	30	21.80 (19.90 – 24.70)	10	18.85 (16.20 – 22.60)	10	20.20 (18.00 – 30.40)

IQR, interquartile range.

theta bursts [31] and slow spindles [27, 28] (Figure 2). During the slow wave upstate, immediately after the trough, we observed EEG activity within broad range of time and frequency space that corresponds to previously-reported fast spindles [20, 27, 28, 31]. Notably, a similarly broad range of upstate-specific spindle activity was previously reported by Muehlroth et al. among older and younger adult subjects, and this upstate spindle composite was referred to as fast and slow spindle activity [20]. We built on these observations, and by implementing methods offering a relatively high frequency resolution of our time-frequency analysis we identified two distinct TF-windows within the slow wave upstate (Figure 2).

Stage N2 and stage N3 slow waves demonstrate distinct compositions of slow wave and sleep spindle coupling

Given that slow wave activity is described to have different functions between stage N2 and stage N3 sleep [51], we sought to characterize populations of slow waves from each sleep stage independently. Notably, the distinction between sleep stages is imperfect, and most often a mixing of lighter and deeper sleep occurs, particularly in transitions between sleep stages [44, 45]. Individual variability of slow waves and spindles has also been demonstrated with regard to frequency and timing aspects of coupling [52], and a well-described misclassification of N3 sleep may occur among older adults as their lower-amplitude slow waves cause N3 to be staged as N2 sleep [44].

Our slow wave detections do indeed demonstrate a trend toward less N3 slow waves and more N2 slow waves with increased age, although the ratio of N2 slow waves/N3 slow waves is largely stable in our observations after the age of 50, indicating that this amplitude-specific misclassification effect does not fully explain age-dependent shifts in slow wave distribution across N2 and N3 sleep (Table 2). Despite these conceptual limitations in the use of AASM sleep staging guidelines, we nonetheless proceeded to use standard definitions of N2 and N3 sleep to divide the spectrum of NREM sleep into "lighter" N2 sleep, and "deeper" N3 sleep given the broad acceptance in the use of AASM sleep staging criteria in the scientific study of sleep and the lack of a validated and broadly-accepted alternative staging method. Using these standard AASM-staged epochs of sleep, we observed that dividing sleep into stages N2 and N3 sleep demonstrated that the overall pattern of slow wave and spindle coupling features is different when comparing the composition of slow waves from stages N2 and N3 sleep (Illustrated in Figure 2; Supplementary Figure S4).

Early-fast spindle coupling is prevalent in the younger years of life

Corresponding to a time period marked by early-life brain maturation, from adolescence to young adulthood, early-fast spindle coupling comprises a relatively high percentage of the total postslow wave (upstate) coupling during stage N2 sleep (Figure 3). To illustrate the prevalence of early-fast spindle coupling in early life (i.e. defined as ages 6–20), we utilized mixed effects models to estimate the percentage of early fast spindle EEG power from the total upstate spindle activity in stage N2 sleep. These early-fast percentages were estimated at age 8 years old (51.16%, 95% CI 50.23% to 52.09%), age

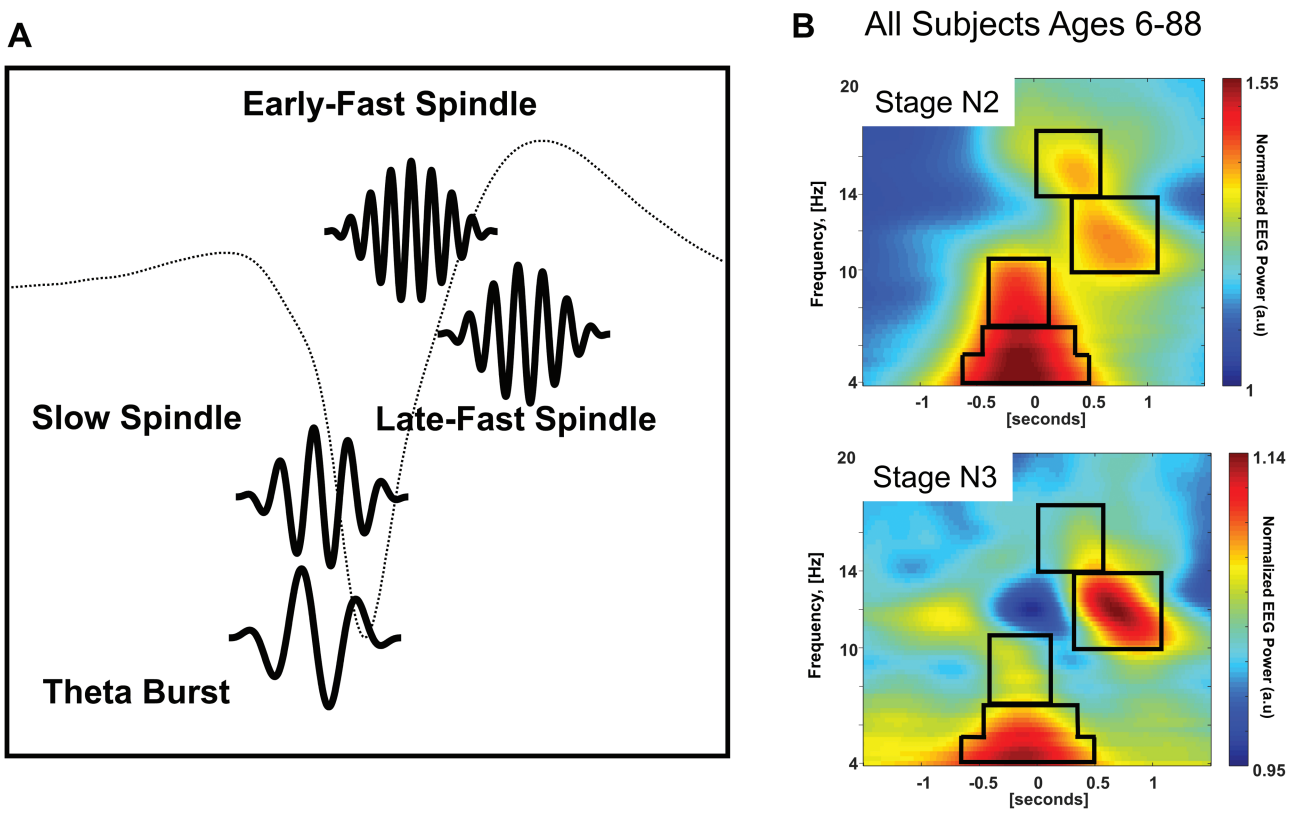

Figure 2. Time-frequency window (TF-window) selection. (A) Four TF-windows were identified a priori (using a separate cohort) as peri-slow wave coupled events. (B) The average of wavelets across all age groups demonstrates differences in relative intensities between stages N2 and N3 wavelets.

13 years old (50.83%, 95% CI 50.27% to 51.39%), and 18 years old (50.51%, 95% CI 50.11% to 50.90%). Subjects within this neurodevelopmental stage also demonstrate a relatively high percentage of early-fast spindle activity in stage N3 sleep (Figure 3B). Stage N3 early-fast spindle TF-window percentages from the statistical model were estimated at age 8 years old (50.09%, 95% CI 49.69% to 50.50%), age 13 years old (49.84%, 95% CI 49.57% to 50.11%), and 18 years old (49.58%, 95% CI 49.34% to 49.83%). Overall comparisons between N2 and N3 sleep among all subjects 6–20 years old also demonstrate a distinction between a higher percentage of early-fast spindles in N2 versus N3 sleep when quantified from corresponding TF windows ($p < 0.001$).

Young adulthood through late life demonstrates a shift in N2 coupling with relative preservation of N3 coupling

We next expanded the scope of age-related coupling changes across the adult portion of the human life cycle (i.e. ages 21 and above). Aging through midlife to late life is associated with a progressive loss of pretrough theta burst and slow spindle activity in N2 sleep (Illustrated from ages 21–80 in Figure 4A; Statistical model in Supplementary Figure S6). The postslow wave percentage of early-fast spindles of stage N2 sleep also progressively declines with age in midlife. Focusing on young adulthood through late adulthood, estimates from our mixed model project a rate of decline at –0.28% early-fast spindle TF-window percentage per 10 years from ages 21–60 years old ($p < 0.001$, 95% CI –0.43% to –0.13%). The shift to a higher percentage of late-fast, postslow wave spindles in stage N2 sleep occurs early in young adulthood, and these late-fast spindles become increasingly predominant posttrough with advancing age (Figure 4A).

Stage N3 sleep demonstrates a moderate decline in early-fast spindle percentage with age (Figure 4C), with an estimated –0.14% change in early-fast spindle percentage per 10 years from ages 21–60 years old ($p = 0.004$, 95% CI –0.23% to –0.04%). Estimated rates of change within early-fast spindle percentages during stages N2 and N3 sleep above age 60 were not statistically significant.

Slow wave subtypes can be separated by their coupling to early-fast and late-fast spindles

We next employed a mechanistic approach to better understand the physiological basis for differences in early-fast and late-fast spindle coupling that we observed at the cohort level. We tested the hypothesis that not all slow waves from our NREM sleep data are fundamentally the same physiological process (i.e. there are distinct subtypes of slow waves that couple with different spindles). We specifically tested whether early-fast and late-fast spindles can be used as an "identification tag" to find and sort distinct subtypes of slow waves.

We focused this approach on a subset of subjects randomly selected from age groups 20–21 years old, 40–41 years old, and 60–61 years old ($n = 30$; ten from each age group) to examine an adult sample representing a broad range of ages across the study population. Starting with a set of heterogeneous slow wave/spindle couples from combined N2 and N3 sleep, we used our defined TF-windows to threshold normalized EEG power and

Table 2. Slow wave amplitudes, numbers, lengths (durations), sleep stage durations, and densities among the study population.

	Ages 6–10	Ages 11–20	Ages 21–30	Ages 31–40	Ages 41–50	Ages 51–60	Ages 61–70	Ages 71–80	Ages 81–88
Number of N2 subjects	22	103	81	50	109	101	43	31	6
Number of N3 subjects	23	106	83	46	104	86	35	18	2
N2 slow wave amplitude	133.18 (26.46)	123.57 (26.8)	107.02 (30.84)	95.42 (31.76)	88.60 (26.95)	89.81 (29.77)	83.56 (29.03)	79.97 (27.24)	61.85 (26.01)
N3 slow wave amplitude	150.70 (28.96)	127.23 (29.89)	97.06 (28.18)	92.27 (34.50)	85.53 (26.31)	88.71 (25.53)	82.09 (32.21)	95.32 (22.30)	88.85 (23.33)
N2 slow wave number	118.14 (98.18)	135.90 (76.02)	175.80 (91.99)	203.18 (134.27)	201.26 (107.12)	208.63 (116.65)	231.19 (141.65)	264.35 (138.28)	235.00 (100.79)
N3 slow wave number	463.74 (123.38)	397.12 (169.59)	301.20 (134.08)	284.48 (163.19)	238.66 (151.31)	249.43 (162.94)	278.74 (163.09)	295.72 (182.21)	295.22 (211.31)
Ratio of N2/N3 slow waves	0.25	0.34	0.58	0.71	0.84	0.84	0.83	0.89	0.80
N2 sleep duration	159.95 (54.57)	187.41 (52.96)	220.25 (31.75)	233.70 (40.20)	219.11 (37.03)	208.14 (37.51)	198.70 (40.33)	191.00 (36.70)	201.83 (45.04)
N3 sleep duration	188.50 (54.04)	129.08 (55.43)	85.30 (31.52)	77.80 (32.43)	70.33 (33.15)	66.95 (33.08)	74.60 (35.02)	56.50 (34.35)	57.56 (38.55)
N2 slow wave events/ minute	0.66 (0.38)	0.71 (0.33)	0.78 (0.30)	0.83 (0.39)	0.90 (0.38)	0.97 (0.43)	1.12 (0.52)	1.36 (0.53)	1.14 (0.37)
N3 slow wave events/ minute	2.59 (0.79)	3.27 (1.21)	3.54 (1.06)	3.66 (1.44)	3.36 (1.36)	3.61 (1.37)	3.72 (1.38)	5.33 (1.56)	5.06 (1.69)
N2 baseline segments	89.27 (60.87)	110.87 (53.81)	144.33 (66.65)	163.66 (94.07)	158.44 (70.01)	163.78 (79.28)	174.74 (86.98)	191.77 (88.05)	235.00 (62.52)
N3 baseline segments	278.00 (58.71)	206.41 (72.38)	151.88 (55.68)	137.63 (55.34)	120.68 (57.84)	120.15 (61.38)	130.09 (60.12)	110.33 (63.74)	130.00 (110.00)
N2 slow wave lengths (durations)	0.76 (0.12)	0.71 (0.078)	0.70 (0.092)	0.73 (0.095)	0.72 (0.085)	0.74 (0.088)	0.74 (0.080)	0.72 (0.053)	0.73 (0.073)
N3 slow wave lengths (durations)	0.66 (0.030)	0.63 (0.054)	0.64 (0.079)	0.68 (0.082)	0.68 (0.081)	0.69 (0.072)	0.72 (0.056)	0.72 (0.047)	0.77 (0.030)

Means (standard deviations) of sleep stage variables; Amplitudes are expressed in microvolts; Duration of sleep stage is expressed in minutes; Slow wave lengths (durations of waves) are expressed in seconds.

separate apart discrete subtypes of slow waves with relatively high coupling activity in each respective TF-window (Figure 5, A–C; Figures 8S and 9S, A–C).

In order to cross-validate this sorting technique and minimize circularity, we next sorted slow wave and spindle coupled pairs using a different signal processing method that does not depend on the TF-window values (i.e. re-creating the spindle "identification tags" without the dependence on time-frequency wavelet data TF-windows). We again utilized the EEG data from combined N2 and N3 sleep from the same 30 subjects aged 20–21, 30–31, and 60–61 years old. The early-fast and late-fast spindles from each recording were first identified as unique events from the raw EEG data. Next, early-fast and late-fast spindle events were assessed for cooccurrences within a time window of –0.5 s to 1.5 s near a downstate trough of a slow wave event (searching for a "match" between slow waves and spindles within this time window). Using this method to "recouple" the early-fast and late-fast spindles with their respective slow waves once again identified distinct populations of slow waves. Comparing the location of these spindles in time and frequency to the previously identified TF-windows, this method produced striking agreement to our original approach with regard to both timing and frequency attributes (Figure 5, D and E; Supplementary Figures S8 and S9, D and E). Of note, subjects in both the 40–41 and 60–61 years old groups demonstrate a mixing of early-fast and late-fast signal when early-fast spindles are identified and recoupled to slow waves, demonstrating the expected technical limitations in completely separating spindle subtypes that share overlapping frequency components with the use of band-pass filter techniques among older subjects who produce relatively less EEG power in the primary frequency components of early-fast spindles (Supplementary Figures S8D and S9D).

Separated slow wave subtypes demonstrate greater late-fast spindle coupling during stage N3 sleep

Having observed that mixed populations of slow waves demonstrate greater late-fast spindle coupling during stage N3 sleep, we next sought to verify this finding among the isolated slow wave subtypes. Using the same subset of thirty subjects, we repeated our separation methods to sort each slow wave by their relative early-fast and late-fast spindle EEG power for stages N2 and N3 sleep independently. We again observed that stages N2 and N3 sleep contain a mix of both coupled slow wave subtypes (Figure 6, A–F; Supplementary Figures S10 and S11, A–F). Notably, the normalized EEG power within the late-fast spindle TF-window is disproportionately high when compared to early-fast spindle TF-window among the slow waves from stage N3 sleep across all ages (Figure 6, F and G; Supplementary Figures S10 and S11, F and G).

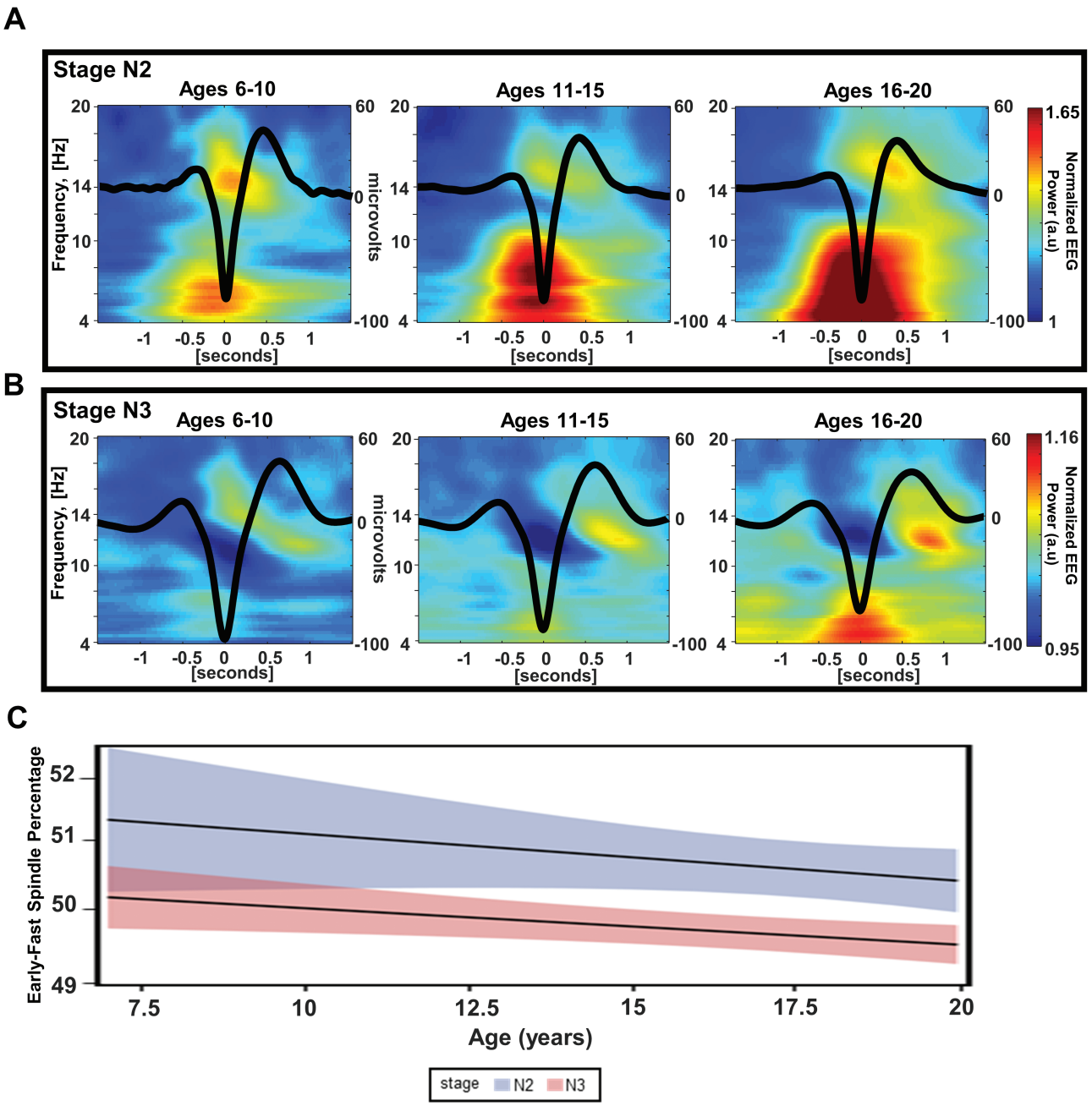

Figure 3. Changes in spindle coupling during childhood and adolescence. (A) Sleep stage N2-specific time-frequency wavelet plots visually illustrate a prominent early-fast spindle signal within the slow wave upstate across multiple age groups. (B) Sleep stage N3-specific time-frequency wavelet plots visually illustrate an increasing intensity of late-fast spindles within the slow wave upstate as age progresses from young children to young adults. Also notable is a relatively intense early-fast spindle signal among subjects aged 6–10 during N3 sleep. (C) Statistical modeling with 95% confidence interval estimation for the percentage of early-fast spindle TF-windows (as a percent of the measured upstate spindle power) through childhood to young adulthood (ages 6–20).

Discussion

Our results support a model in which distinct subtypes of spindle coupling extend beyond the "slow" and "fast" subtypes that were originally described [27, 28]. The existence of two distinct, temporally dissociated, spindles postslow wave trough (during the upstate of the slow wave) has been reported from intracranial recordings [31, 32], and Andrillon et al. described these events as "fast" and "slow" spindles [32], while Gonzalez et al. labeled them "faster" and "slower" spindles [31]. Muehlroth el al. similarly reported the coupling of both "fast" and "slow" spindles occurs during the slow wave upstate in surface EEG [20]. Here we reproduce these findings, characterizing two distinct coupled spindle events postslow wave trough, within the upstate region. Notably, we avoided referring to spindles within the slow wave upstate as "slow" spindles due to confusing terminology that has been used to apply the label of "slow" to coupled spindles within the upstate [20, 32], in addition to coupled spindles within the downstate (near the slow wave trough) [20, 27], and to spindle events studied without assessment of coupling during NREM sleep [53–56]. We have instead

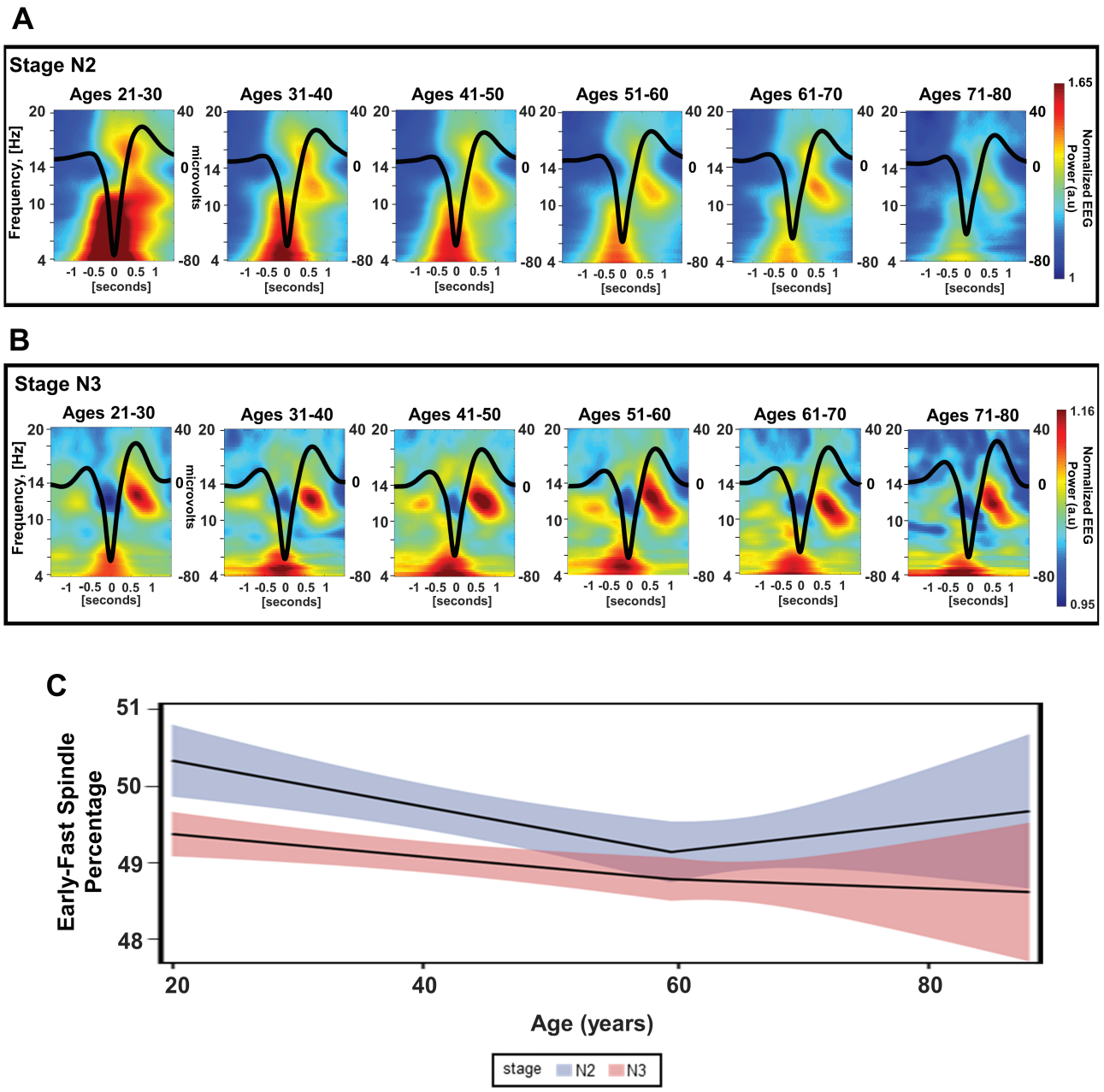

Figure 4. Changes in spindle coupling during young adulthood through late age. (A) Sleep stage N2-specific time-frequency wavelet plots visually illustrate the relative amount of each peri-slow wave event across multiple age groups. (B) Sleep stage N3-specific time-frequency wavelet plots visually illustrate the relative amount of each peri-slow wave event across multiple age groups. (C) Statistical modeling with 95% confidence interval estimation for the percentage of early-fast spindle TF-windows (as a percent of the measured upstate spindle power) through childhood to young adulthood (ages 21–88).

referred to the two upstate-specific spindle events as "early-fast" and "late-fast" spindles in accordance with their respective timing aspects to the slow wave trough. Consistent with prior reports [20, 31, 32], we demonstrate that the early-fast subtype occurs closer to the slow wave trough, at the beginning of the upstate, while the late-fast subtype is maximal closer to the peak of the upstate.

We further report that both stage N2 and N3 sleep contain a composite of early-fast and late-fast coupling subtypes. Despite the presence of mixed subtypes, the relative amount of different coupling subtypes within each sleep stage can be reliably measured, is age dependent, and demonstrates a continuum across the human life span. Childhood and adolescence are associated with relatively higher early-fast spindle coupling, whereas the late-fast postslow wave trough coupling subtype becomes increasingly predominant through midlife and into the later stages of life. We further provide compelling mechanistic data demonstrating that the coupling of different spindle subtypes can be used to identify distinct slow wave subtypes during both N2 and N3 sleep.

The coordinated coupling of slow waves and sleep spindles provides a conceptual framework for understanding sleep's role in synaptic regulation and memory consolidation [18]. Among the most challenging gaps in this framework are the conflicting

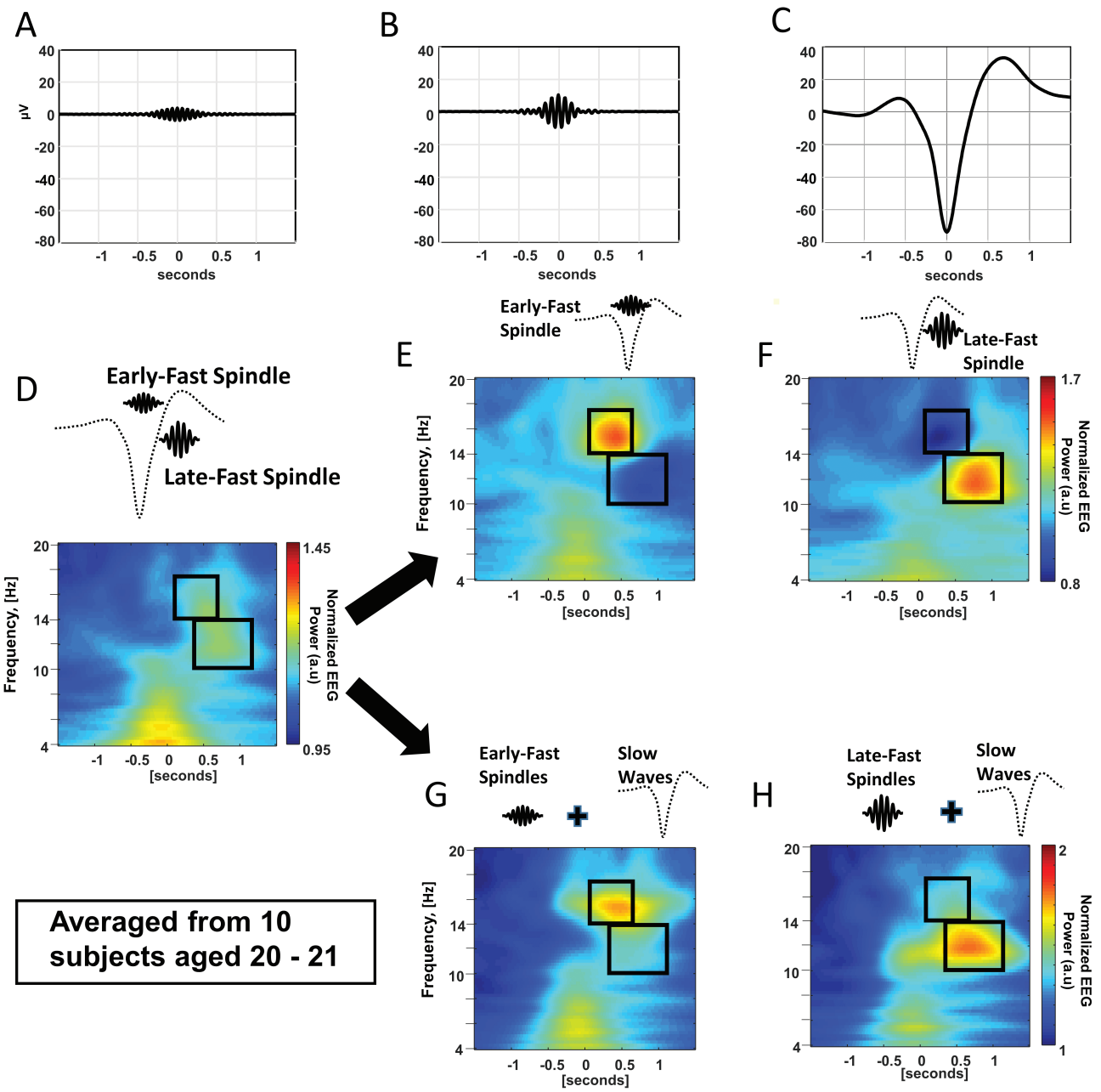

Figure 5. Two methods are used to cross-validate separation of distinct slow wave and spindle coupling pairs (Data averaged from 10 subjects, ages 20–21 years old). (A) The average EEG time-series signal of early-fast spindles that were detected and used for subsequent analysis. The average spindle composite is centered on $t = 0$ for illustrative purposes. (B) The average EEG time-series signal of late-fast spindles that were detected and used for subsequent analysis. The average spindle composite is centered on $t = 0$ for illustrative purposes. (C) The average EEG time-series signal of slow wave events that were detected and used for subsequent analysis. The average slow wave composite is centered on $t = 0$ for illustrative purposes. (D) The relative spatial location of early-fast and late-fast spindles with regard to slow waves is illustrated (upper; not to scale). The combined N2 and N3 average composite of slow wave time-frequency wavelets maps are graphed with TF-windows referencing the early-fast and late-fast spindle locations. (E and F) Slow waves coupled to early-fast and late-fast spindles were enriched by their relatively high power within the respective TF-windows. Note that upper illustrations of spindle and slow wave shapes are not to scale. (G and H) Early-fast and late-fast spindle events were first identified independently from EEG time-series data (as graphed in A and B), then used to identify their respective coupled slow wave events by matching spindles to slow waves that occur –0.5 s to 1.5 s from the trough of each slow wave. TF-windows are depicted for reference of early-fast and late-fast spindle locations. Note that upper illustrations of spindle and slow wave shapes are not to scale.

findings as to whether coupled spindles are responsible for potentiating vs downscaling synaptic strength [57]. More current models that seek to reconcile these seemingly opposing findings propose that synapses are selectively downscaled or potentiated by distinct mechanisms during NREM sleep [58, 59]. Indeed, a study by Kim et al. recently demonstrated in murine sleep that two subclasses of slow wave and spindle coupling demonstrate opposing effects in synaptic potentiation vs downscaling. This study further reported that globally-occurring slow wave and spindle coupling is associated with synaptic potentiation, while the local subtype of slow wave and spindle coupling drives downscaling [35].

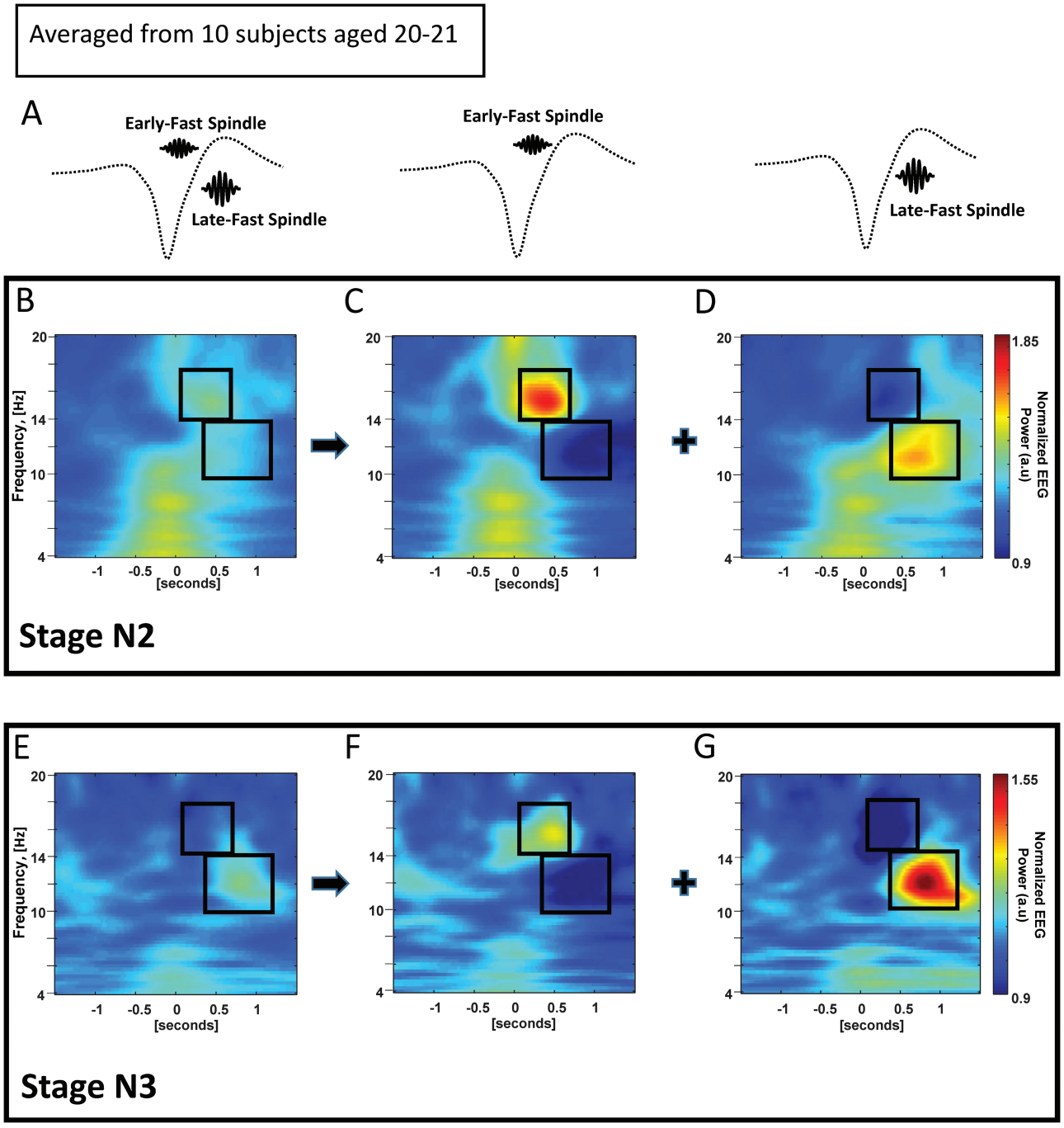

Figure 6. Sleep stage specific slow wave sorting (Data averaged from 10 subjects, ages 20–21 years old). (A) An illustration of coupled spindles depicts mixed slow waves on the left, versus slow waves separated by their coupling to spindles in the middle and right panels. Note that spindle and slow wave shapes are not drawn to scale. (B–D) Slow waves were identified by their coupling to early-fast or late-fast spindle subtypes by TF-window and separated into two distinct slow wave populations from stage N2 sleep. (E–G) Slow waves were identified by their coupling to early-fast or late-fast spindle subtypes by TF-window and separated into two distinct slow wave populations from stage N3 sleep.

While a human equivalent of this dual system of opposing synaptic regulation has not been identified, human NREM sleep does contain a mix of global and local slow wave events [33, 34]. Global events, also termed Type I slow waves, have been suggested to represent K complexes and are generated independent of local sleep pressure [33, 34]. Local, Type II, slow wave events demonstrate a dynamic correlation to ongoing homeostatic sleep pressure and are thought to be "delta waves" of deeper stage N3 sleep [33]. Although our analyses are not able to attribute global versus local characteristics to slow wave and spindle coupling subtypes, we do observe a distinction between the prevalence of discrete coupling subtypes throughout lighter N2 and deeper N3 sleep. Future studies will be required to determine whether early-fast and late-fast subtypes of spindle coupling may have specificity to global or local slow wave event subtypes.

Changes in slow wave and spindle coupling relationships have been shown to correlate with performance on overnight memory consolidation, and age-dependent loss of coupling is associated with poorer performance on these memory tasks [20, 21]. Our analyses suggest that changes in this neuronal circuitry occur across the human lifespan. Childhood is marked by relatively higher early-fast spindle EEG power in both stages N2 and N3 sleep, with a progressive decline through adolescence; although we cannot infer causality based on our study design, it is possible that this reflects neurodevelopmental changes in synaptic regulation. Further, we observe shifts in coupling as a progression from young adulthood through old age, and these changes may reflect a continuum sleep physiology's contributions to well-documented lifelong changes in memory functions [60].

Degradation of coupled spindle timing may signal neuronal dysfunction early in the pathogenesis of Alzheimer's disease [22], raising prospects of developing a coupling-based functional biomarker of disease pathology. Our finding that distinct subclasses of slow waves can be separated by their spindle coupling provides a mechanistic framework to further develop these biomarker methods. In particular, we observe that early-fast and late-fast spindles have frequency overlap near the peak frequency for all spindle events, around 14 Hz, and therefore implementation of bandpass filters that share this frequency window may inadvertently mix both early-fast and late-fast spindle events. Given the distinct timing aspects of early-fast and late-fast spindles with regard to their respective slow wave downstate troughs and upstate peaks, this mixing of spindle events may complicate the interpretation of spindle timing measurements.

Aging is associated with decreased amplitude of slow waves [44, 61], and changes in slow wave morphology have also been described with increasing age [62]. The decrement in slow wave amplitude among older adults also produces a well-described loss of stage N3 sleep scoring; this is due, in part, to technical limitations with the use of an absolute slow wave size threshold rule for scoring that causes segments of NREM sleep to be labeled as stage N2 instead of N3 sleep [40, 44]. Unfortunately, to date there is no consensus regarding a precise age range at which N3 sleep might be "misclassified" as N2 sleep, although a recent report by Muehlroth and Werkle-Bergner suggests the among young adults (examined between ages 19–28 years old), there is negligible concern for misclassification, while ~60% of older adults (examined between ages 63–74 years old) might have an appreciable amount of this N3-to-N2 misclassification [44]. Notably, these limitations are inherent in all studies of sleep that rely on drawing a distinction between N2 and N3 sleep among subjects where misclassification may occur.

Our own data suggest that slow wave amplitudes do not drop to a range that would raise concern for possible N3 sleep misclassification until somewhere between 30 and 40 years old, and the ratio of slow waves detected in N2 versus N3 sleep is relatively stable starting between the ages of 40 and 50 years old (see Table 2). Further, while there is a possibility for this misclassification to occur among subjects after the age of 30, the rate of decline in average slow wave amplitudes suggests that the risk of misclassification is minimal among subjects in their 30s and 40s. Notably, our data demonstrate that the predominant slow waves become "N3-like" (N2 sleep becomes increasingly filled by slow waves with a coupling pattern of predominantly late-fast spindles) much earlier in life than N3 misclassification likely occurs, and this effect is observable across hundreds of subjects who are younger than 30 years old and thus would not be expected to have any significant problems with misclassification. Critically, despite the need to contextualize these important technical limitations, the broader interpretation and scientific implications of our data do not rely on an immediate accounting for how N2-like waves may be "disappearing" among the elderly. To the contrary, our demonstration that a substantial number of N3-like slow waves "take over" the amalgam of stage N2 sleep across the human lifespan is a remarkable observation, regardless of how this state comes to be (i.e. the loss of N2-like waves versus a shift in N3-like waves to the N2 sleep).

This pattern of N2-like slow wave coupling loss with increasing age is also suggested in our "recoupling" of slow wave with spindles, and in our separation of slow waves by their spindles using normalized TF-window EEG power, both having been performed within subanalyses that utilized pooled N2 and N3 data (as illustrated in Figure 5; Supplementary Figures S8 and S9). As these subanalyses were not structured to provide quantitative differences across ages, this observation should be considered as a preliminary finding within the context of these specific subanalysis methods. Consequently, future studies will be required to better describe the precise neurophysiological mechanisms underlying our observations, and these studies may benefit from a methodological shift to the conceptualization of sleep stages as a continuum, as Muehlroth and Werkle-Bergner have proposed as a means address the complex technical challenges in staging sleep among older adults [44].

In addition to early-fast and late-fast spindles, events occurring prior to the trough of the slow wave downstate include the originally described slow spindles [27, 47, 48] and the more recently described theta bursts [29–31]. While little is known about the function of these pretrough coupled slow spindles, theta bursts are proposed to trigger slow wave events [29–31], and may also precede hippocampal ripples during memory consolidation [29, 30]. Notably, the ability to clearly distinguish between these pretrough events is somewhat limited by surface EEG, and indeed Gonzalez et al. have questioned whether the pretrough (downstate) slow spindle might be simply an extension of the theta burst [31]. Nonetheless, our data demonstrating a separation of slow wave events by spindle coupling suggest that pretrough theta bursts and slow spindles might be more frequently associated with early-fast spindle-coupled slow wave events (Figure 5; Supplementary Figures S8 and S9). Notably, theta bursts typically precede slow waves and K-complexes of stage N2, and are less likely to precede slow waves of stage N3 sleep [31]. Thus, although somewhat speculative, these observations suggest another possible link to a global (light sleep) vs local (deep sleep) relationship with distinct subtypes of slow wave and spindle coupling.

One of the strengths of our study is the utilization of a large sample size to find consistencies in slow waves and spindle coupling amongst the great individual variability that we and others have observed [52]. This variability is also a limitation of our approach, in that we remain unable to precisely quantify different subtypes of slow waves and spindles at the single-subject level given variability in both frequency and timing of these events between individuals. These issues are further exacerbated among aging adults, where the overlapping frequency ranges of early-fast and late-fast spindles create

technical challenges in separating these events into discrete subpopulations, particularly as the relative of EEG power in the frequency range of late-fast spindles becomes increasingly disproportionate (Supplementary Figures S9). Further, our experience aligns with other studies in that we find many spindles and slow waves do not demonstrate coupling when analyzed from surface EEG (illustrated in Supplementary Figure S2) [27, 46, 52]. These limitations remain one of the major barriers to the development of this technique as functional biomarker that could be used to predict neurodegenerative disease within an individual aging adult. Future work will be needed to identify additional defining attributes of slow waves and spindles and to refine individualized sorting methods for more consistent quantification of coupling subtypes.

Another technical aspect to consider is our selection of baseline segments for normalization of EEG power, which is necessary to measure changes in EEG power that are specific to slow wave events against the background of ongoing brain activity. As we visually illustrate in Supplementary Figure S2, and as noted by others who have characterized sleep spindles [27, 32, 46], EEG activity is prominent within the frequency bands that define spindles, and much of the EEG power in these frequency bands is not attributable to specific spindle events. Our coupling analyses were performed to maximize specificity in the quantification of the EEG power that can be attributed to coupled spindles. Similar to prior studies of slow wave and spindle coupling [20, 28], we focused on slow wave-coupled EEG power by estimating the EEG power changes during slow wave events in comparison to baseline EEG activity near the time of slow wave events, Further, uncoupled spindles are abundant during NREM sleep [27, 32, 46], and while our assessment of coupled spindles accounts for their average contribution to the EEG power of ongoing brain activity, we are unable to make direct comparisons between coupled and uncoupled spindles within our analyses. These limitations are further complicated by the tendency for spindles to occur in clusters that may result in more than one spindle overlapping with a single slow wave event. Future studies will be required to better differentiate and characterize the properties of uncoupled spindles from the events that are specifically coupled to slow waves, which is particularly relevant to the use of the terms “fast” and “slow” to describe numerous types of spindle events with varying time and frequency characteristics [20, 27, 28, 31, 32, 46, 49, 52, 54–56, 63].

Conclusion

In conclusion, we find that human NREM sleep contains an amalgam of distinct slow wave and spindle coupling events that mix together to form composites of slow wave sleep. Clear separation of stages N2 and N3 sleep presents some challenges across all ages, but classifying sleep stage epochs by AASM criteria does demonstrate that each stage contains differing amounts of early-fast spindles versus late-fast spindles, possibly reflecting distinctions in the function of slow wave subtypes between the stages of sleep. The composition of slow wave and spindle subtypes can be observed to transition across phases of the human life cycle, and a pattern of deeper sleep coupling is progressively predominant with increased age beginning in the later stages of childhood. These insights provide a conceptual foundation to advance our knowledge of sleep's memory functions. Finally, several clinically relevant advancements may come from these observations in both efforts to utilize slow wave and spindle physiology as a biomarker for detection of early Alzheimer's disease [22, 64, 65] and ongoing clinical trials aiming to restore or enhance slow wave sleep as a clinical intervention [25, 66, 67].

Supplementary material

Supplementary material is available at *SLEEP* online.

Funding

The authors are grateful for the open access to data provided by the Cleveland Family Study (CFS) (supported by grants from the National Institutes of Health (HL46380, M01 RR00080-39, T32-HL07567, RO1-46380)), and the National Sleep Research Resource (supported by the National Heart, Lung, and Blood Institute (R24 HL114473, RFP 75N92019R002)). A portion of this research was also supported by a grant from the American Academy of Neurology and the McKnight Brain Institute.

Author Contributions

B.V.M., E.K., P.D.T, S.H.S, A.J.F., A.R.D., A.R.R, R.L.M. and B.M.B. designed the study; B.V.M., S.H.S, G.M.F., R.I.K., A.J.F., A.R.D. and M.W.B. analyzed the data; B.V.M. and B.M.B. wrote the manuscript; E.K., P.D.T., A.R.R., and B.D.B. gave conceptual advice. All authors participated in editing and revision of the manuscript.

Disclosure Statement

None declared.

Data Availability

The data underlying this article are available in the National Sleep Research Resource, at https://sleepdata.org/. A draft of this manuscript was this manuscript was uploaded to the preprint repository BioRxiv doi: https://doi.org/10.1101/2020.05.28.122168

References

1. Contreras D, *et al*. Cellular basis of EEG slow rhythms: a study of dynamic corticothalamic relationships. *J Neurosci*. 1995;**15**(1 Pt 2):604–622.
2. Steriade M, *et al*. Slow sleep oscillation, rhythmic K-complexes, and their paroxysmal developments. *J Sleep Res*. 1998;**7 Suppl 1**:30–35.
3. Sanchez-Vives MV, *et al*. Cellular and network mechanisms of rhythmic recurrent activity in neocortex. *Nat Neurosci*. 2000;**3**(10):1027–1034.
4. von Krosigk M, *et al*. Cellular mechanisms of a synchronized oscillation in the thalamus. *Science*. 1993;**261**(5119): 361–364.
5. McCormick DA, *et al*. Brain state dependent activity in the cortex and thalamus. *Curr Opin Neurobiol*. 2015;**31**:133–140.
6. Ju YES, *et al*. Sleep and Alzheimer disease pathology—a bidirectional relationship. *Nat Rev Neurol*. 2014;**10**(2):115.

7. Niethard N, *et al*. Cortical circuit activity underlying sleep slow oscillations and spindles. *Proc Natl Acad Sci U S A*. 2018;**115**(39):E9220–E9229.
8. Ulrich D. Sleep spindles as facilitators of memory formation and learning. *Neural Plast*. 2016;**2016**:1796715.
9. Antony JW, *et al*. Sleep spindles and memory reprocessing. *Trends Neurosci*. 2019;**42**(1):1–3.
10. Cairney SA, *et al*. Memory consolidation is linked to spindle-mediated information processing during sleep. *Curr Biol*. 2018;**28**(6):948–954.e4.
11. Antony JW, *et al*. Sleep spindle refractoriness segregates periods of memory reactivation. *Curr Biol*. 2018;**28**(11):1736–1743.e4.
12. Girardeau G, *et al*. Hippocampal ripples and memory consolidation. *Curr Opin Neurobiol*. 2011;**21**(3):452–459.
13. Siapas AG, *et al*. Coordinated interactions between hippocampal ripples and cortical spindles during slow-wave sleep. *Neuron*. 1998;**21**(5):1123–1128.
14. Sirota A, *et al*. Communication between neocortex and hippocampus during sleep in rodents. *Proc Natl Acad Sci U S A*. 2003;**100**(4):2065–2069.
15. Battaglia FP, *et al*. Hippocampal sharp wave bursts coincide with neocortical "up-state" transitions. *Learn Mem*. 2004;**11**(6):697–704.
16. Mölle M, *et al*. Hippocampal sharp wave-ripples linked to slow oscillations in rat slow-wave sleep. *J Neurophysiol*. 2006;**96**(1):62–70.
17. Diekelmann S, *et al*. The memory function of sleep. *Nat Rev Neurosci*. 2010;**11**(2):114–126.
18. Moelle M, *et al*. Slow oscillations orchestrating fast oscillations and memory consolidation. *Prog Brain Res*. 2011;**193**:93–110.
19. Abel T, *et al*. Sleep, plasticity and memory from molecules to whole-brain networks. *Curr Biol*. 2013;**23**(17):R774–R788.
20. Muehlroth BE, *et al*. Precise slow oscillation-spindle coupling promotes memory consolidation in younger and older adults. *Sci Rep*. 2019;**9**(1):1940.
21. Helfrich RF, *et al*. Old brains come uncoupled in sleep: slow wave-spindle synchrony, brain atrophy, and forgetting. *Neuron*. 2018;**97**(1):221–230.e4.
22. Winer JR, *et al*. Sleep as a potential biomarker of Tau and β-Amyloid burden in the human brain. *J Neurosci*. 2019;**39**(32):6315–6324.
23. Rosanova M, *et al*. Pattern-specific associative long-term potentiation induced by a sleep spindle-related spike train. *J Neurosci*. 2005;**25**(41):9398–9405.
24. Fogel SM, *et al*. The function of the sleep spindle: a physiological index of intelligence and a mechanism for sleep-dependent memory consolidation. *Neurosci Biobehav Rev*. 2011;**35**(5):1154–1165.
25. Mander BA, *et al*. Sleep: a novel mechanistic pathway, biomarker, and treatment target in the pathology of Alzheimer's Disease? *Trends Neurosci*. 2016;**39**(8):552–566.
26. Cordone S, *et al*. Sleep and β-amyloid deposition in Alzheimer disease: insights on mechanisms and possible innovative treatments. *Front Pharmacol*. 2019;**10**:695.
27. Mölle M, *et al*. Fast and slow spindles during the sleep slow oscillation: disparate coalescence and engagement in memory processing. *Sleep*. 2011;**34**(10):1411–1421. doi: 10.5665/SLEEP.1290
28. Klinzing JG, *et al*. Spindle activity phase-locked to sleep slow oscillations. *Neuroimage*. 2016;**134**:607–616.
29. Jiang X, *et al*. Coordination of human hippocampal sharpwave ripples during NREM sleep with cortical theta bursts, spindles, downstates, and upstates. *J Neurosci*. 2019;**39**(44):8744–8761.
30. Jiang X, *et al*. Posterior hippocampal spindle ripples co-occur with neocortical theta bursts and downstates-upstates, and phase-lock with parietal spindles during NREM sleep in humans. *J Neurosci*. 2019;**39**(45):8949–8968.
31. Gonzalez CE, *et al*. Theta bursts precede, and spindles follow, cortical and thalamic downstates in human NREM Sleep. *J Neurosci*. 2018;**38**(46):9989–10001.
32. Andrillon T, *et al*. Sleep spindles in humans: insights from intracranial EEG and unit recordings. *J Neurosci*. 2011;**31**(49):17821–17834.
33. Bernardi G, *et al*. Local and widespread slow waves in stable NREM sleep: evidence for distinct regulation mechanisms. *Front Hum Neurosci*. 2018;**12**:248.
34. Siclari F, *et al*. Two distinct synchronization processes in the transition to sleep: a high-density electroencephalographic study. *Sleep*. 2014;**37**(10):1621–1637. doi: 10.5665/sleep.4070
35. Kim J, *et al*. Competing roles of slow oscillations and delta waves in memory consolidation versus forgetting. *Cell*. 2019;**179**(2):514–526.e13.
36. Dean DA 2nd, *et al*. Scaling up scientific discovery in sleep medicine: The National Sleep Research Resource. *Sleep*. 2016;**39**(5):1151–1164. doi: 10.5665/sleep.5774
37. Zhang GQ, *et al*. The National Sleep Research Resource: towards a sleep data commons. *J Am Med Inform Assoc*. 2018;**25**(10):1351–1358.
38. Redline S, *et al*. The familial aggregation of obstructive sleep apnea. *Am J Respir Crit Care Med*. 1995;**151**(3 Pt 1):682–687.
39. Redline S, *et al*. Risk factors for sleep-disordered breathing in children. Associations with obesity, race, and respiratory problems. *Am J Respir Crit Care Med*. 1999;**159**(5 Pt 1):1527–1532.
40. Berry RB, *et al*. *The AASM Manual for the Scoring of Sleep and Associated Events. Rules, Terminology and Technical Specifications*. Darien, IL: American Academy of Sleep Medicine; 2012.
41. Delorme A, *et al*. EEGLAB: an open source toolbox for analysis of single-trial EEG dynamics including independent component analysis. *J Neurosci Methods*. 2004;**134**(1):9–21.
42. Oostenveld R, *et al*. FieldTrip: open source software for advanced analysis of MEG, EEG, and invasive electrophysiological data. *Comput Intell Neurosci*. 2011;**2011**:156869.
43. Prerau MJ, *et al*. Sleep neurophysiological dynamics through the lens of multitaper spectral analysis. *Physiology (Bethesda)*. 2017;**32**(1):60–92.
44. Muehlroth BE, *et al*. Understanding the interplay of sleep and aging: methodological challenges. *Psychophysiology*. 2020;**57**(3):e13523.
45. Younes M, *et al*. Staging sleep in polysomnograms: analysis of inter-scorer variability. *J Clin Sleep Med*. 2016;**12**(6):885–894.
46. Mölle M, *et al*. Grouping of spindle activity during slow oscillations in human non-rapid eye movement sleep. *J Neurosci*. 2002;**22**(24):10941–10947.
47. De Gennaro L, *et al*. Sleep spindles: an overview. *Sleep Med Rev*. 2003;**7**(5):423–440.
48. Anderer P, *et al*. Low-resolution brain electromagnetic tomography revealed simultaneously active frontal and parietal sleep spindle sources in the human cortex. *Neuroscience*. 2001;**103**(3):581–592.
49. Cox R, *et al*. Individual differences in frequency and topography of slow and fast sleep spindles. *Front Hum Neurosci*. 2017;**11**:433.

50. Staresina BP, *et al*. Hierarchical nesting of slow oscillations, spindles and ripples in the human hippocampus during sleep. *Nat Neurosci*. 2015;**18**(11):1679–1686.
51. Genzel L, *et al*. Light sleep versus slow wave sleep in memory consolidation: a question of global versus local processes? *Trends Neurosci*. 2014;**37**(1):10–19.
52. Cox R, *et al*. Large-scale structure and individual fingerprints of locally coupled sleep oscillations. *Sleep*. 2018;**41**(12). doi: 10.1093/sleep/zsy175
53. Fogel S, *et al*. Sleep spindles: a physiological marker of age-related changes in gray matter in brain regions supporting motor skill memory consolidation. *Neurobiol Aging*. 2017;**49**:154–164.
54. Purcell SM, *et al*. Characterizing sleep spindles in 11,630 individuals from the National Sleep Research Resource. *Nat Commun*. 2017;**8**:15930.
55. Zeitlhofer J, *et al*. Topographic distribution of sleep spindles in young healthy subjects. *J Sleep Res*. 1997;**6**(3): 149–155.
56. Ayoub A, *et al*. Differential effects on fast and slow spindle activity, and the sleep slow oscillation in humans with carbamazepine and flunarizine to antagonize voltage-dependent Na+ and Ca2+ channel activity. *Sleep*. 2013;**36**(6):905–911. doi: 10.5665/sleep.2722
57. Timofeev I, *et al*. Sleep slow oscillation and plasticity. *Curr Opin Neurobiol*. 2017;**44**:116–126.
58. Puentes-Mestril C, *et al*. Linking network activity to synaptic plasticity during sleep: hypotheses and recent data. *Front Neural Circuits*. 2017;**11**:61.
59. Klinzing JG, *et al*. Mechanisms of systems memory consolidation during sleep. *Nat Neurosci*. 2019;**22**(10):1598–1610.
60. Park DC, *et al*. Theories of memory and aging: a look at the past and a glimpse of the future. *J Gerontol B Psychol Sci Soc Sci*. 2017;**72**(1):82–90.
61. Carrier J, *et al*. Sleep slow wave changes during the middle years of life. *Eur J Neurosci*. 2011;**33**(4):758–766.
62. Ujma PP, *et al*. Individual slow-wave morphology is a marker of aging. *Neurobiol Aging*. 2019;**80**:71–82.
63. Schabus M, *et al*. Hemodynamic cerebral correlates of sleep spindles during human non-rapid eye movement sleep. *Proc Natl Acad Sci U S A*. 2007;**104**(32):13164–13169.
64. Kam K, *et al*. Sleep oscillation-specific associations with Alzheimer's disease CSF biomarkers: novel roles for sleep spindles and tau. *Mol Neurodegener*. 2019;**14**(1):10.
65. Lucey BP, *et al*. Reduced non-rapid eye movement sleep is associated with tau pathology in early Alzheimer's disease. *Sci Transl Med*. 2019;**11**(474):eaau6550.
66. Minakawa EN, *et al*. Sleep disturbance as a potential modifiable risk factor for Alzheimer's disease. *Int J Mol Sci*. 2019;**20**(4):803.
67. Léger D, *et al*. Slow-wave sleep: from the cell to the clinic. *Sleep Med Rev*. 2018;**41**:113–132.